DOE/ET-53088-94 IFSR #94

LOOP COALESCENCE IN FLARES AND CORONAL X-RAY BRIGHTENING

T. Tajima and F. Brunel
Department of Physics and Institute for Fusion Studies
The University of Texas at Austin
Austin, TX 78712
and
J. Sakai
National Center for Atmospheric Research
High Altitude Observatory
Boulder, CO 80307

May 1983

LOOP COALESCENCE IN FLARES AND CORONAL X-RAY BRIGHTENING

T. Tajima and F. Brunel

Department of Physics and Institute for Fusion Studies

University of Texas

Austin, TX 78712

and

J. Sakai

National Center for Atmospheric Research

High Altitude Observatory

Boulder, CO 80307

Characteristics of solar flares such as their impulsive nature, time scale, heating, high energy particle spectrum, γ-ray oscillations as well as recent x-ray photographs of coronal brightening are explained by the nonlinear coalescence instability of current loops.

I. Introduction

Recent direct observation in soft x-rays (Howard and Svestka, 1977) of interconnecting coronal loops spurs the theorist to consider the loop coalescence as an important process for solar flares and coronal x-ray brightening phenomena. Another recent observation (Forrest et al., 1981) of amplitude oscillations in gamma ray emission from the impulsive phase of a solar flare adds curiosity and an important clue to the underlying physical process. We propose in this Letter that the nonlinear development of the coalescence instability of current loops provides a coherent explanation of the above observations. The present theory also offers a quantitative and natural explanation of such known characeristics as the impulsive nature of flares, the time scale of the impulsive phase, intense heating by flares, and formation of high energy tail of particle distribution. Much of observational data as well as models (e.g. Gold and Hoyle, 1960) for solar flares are reviewed in a recent Skylab Solar Workshop (Sturrock, 1980). (See also Svestka, 1976).

As is well known, the annihilation of magnetic energy and its conversion into kinetic one by the tearing instability (Furth et al., 1963) are too slow to account for the present problem. Many authors (Sweet, 1958; Parker, 1963; Petschek, 1964) have proposed fast magnetic reconnection mechanisms. Recently Tajima (1981) found that the reconnection rate for a compressible plasma with weak toroidal magnetic field B_t is much larger (by a factor $10^2 \sim 10^3$) than that for a nearly incompressible plasma with large B_t and that the sharp transition in reconnection behavior takes place when the poloidal field B_p (created by the field aligned current J_t) exceeds

approximately B_t. Brunel et al. (1982) found further that when the plasma is compressible a faster second phase of reconnection sets in after one Alfven time of the Sweet-Parker first phase with reconnected flux

$$\psi = \psi_{SP}(t_A) \cdot (t/t_A)^{\rho_i/\rho_e} \quad , \tag{1}$$

where ψ_{SP} is the Sweet-Parker flux

$$\psi_{SP}(t) = \eta^{1/2} B_p(y=a)(\rho_i/\rho_e)^{1/2}(v_{Al}L)^{1/2}\, t,$$

ρ_i and ρ_e are densities inside and outside of the current channel ($\rho_i \geq \rho_e$), t_A the Alfven time ($t_A = a/v_{Al} = a\sqrt{4\pi\rho}/B_p$), η the resistivity, a the current channel width, and L the length of reconnecting region. According to our theory the reconnection of flux proceeds much faster ($\psi \propto t^{\rho_i/\rho_e}$) than the Sweet-Parker rate ($\psi \propto t$), where for compressible plasmas $\rho_i/\rho_e > 1$. When the plasma has a strong toroidal field and the plasma is incompressible, the reconnection rate reduces to the Sweet-Parker rate even for $t > t_A$. The theory is in good agreement with our computer simulation results (Brunel et al. 1982; Tajima, 1981). Nevertheless the reconnection process in itself, however fast it is, is not responsible for the large magnetic energy conversion into the particle energy, but rather the change in the magnetic geometry from before to after the reconnection process is. Indeed only a small fraction of the total poloidal magnetic energy is released through the reconnection process which necessarily take place at the x-point, i.e. the field null point, where not much magnetic energy is available in the first place.

It is the nonlinear development of the coalescence instability of the current filaments (loops) that can release a large amount of magnetic energy (Wu et al. 1981; Leboeuf et al. 1981). Although the coalescence instability is of ideal magnetohydrodynamic (MHD) nature in the linear stage and the growth rate for compressible plasmas is somewhat smaller than that for incompressible cases (Pritchett et al., 1979), the nonlinear development of this instability involves field line reconnection and therefore is of nonideal MHD nature. Since the reconnection rate drastically differs by two or three orders of magnitude (Tajima, 1981), the nonlinear coalescence time differs by two or three orders of magnitude for case $B_p \gtrsim B_t$ and case $B_p \lesssim B_t$. We studied the coalescence of two current filaments in detail using analytical and computer simulation techniques.

II. Computer Simulation and Theory

A plasma configuration which is unstable against the tearing and subsequent coalescence instabilities is studied by fully self-consistent electromagnetic relativistic particle simulation code (Langdon et al., 1976; Lin et al., 1974). Figure 1 shows a typical field line pattern after the coalescence process begins to proceed. When the linear stage is past and two magnetic islands (i.e. current filaments) approach, the islands are squashed. By this time, the crossing angle α of the separatrix [Fig. 1(b)] decreases until the Sweet-Parker condition [current sheet formation, Fig. 1(c)] is realized. When the plasma is compressible, the crossing angle α then tries to increase [current sheet fans out, Fig. 1(d)] because the process enters in the second phase of reconnection (Brunel et al.,

1982) and this quickly converts the separated island flux into common coalesced flux [see model sketch Fig. 1(b)-(d)]. The plasma near the contact area of islands is squeezed and has a high density, which leads to fast reconnection according to Eq. (1). Because of this, the total flux reconnection of two islands into a coalesced island takes place only within $1 \sim 2$ Alfven times according to our simulation.

The magnetic energy contained in the island fields is explosively released into ion kinetic energy as seen in Fig. 2(a). The amount of energy available W_c by attracting two toroidal current rods I of radius a with separation L is

$$W_c = \frac{2I^2}{c^2} \ell n \frac{L}{a} \quad . \tag{2}$$

Our simulation shows that about 1/6 of energy W_c was transferred to kinetic energy upon coalescence in the case of $B_t = 0$. This amount of energy conversion during 3 is many orders of magnitude larger than is released during the tearing process 1 [see Fig. 2(a)]. The ion temperature shown in Fig. 2(a) sharply increases upon the nonlinear coalescence stage in $1 \sim 2$ Alfven times. Significantly, there appear amplitude oscillations in the temperature, whose frequency matches $\omega \simeq k_\perp v_{A\perp}$, where $k_\perp = 2\pi/a$. This temperature oscillation behavior can be attributed to the overshooting of coalescing and colliding two current blobs. Once two current blobs coalesce, they are bound by the common magnetic flux and the coalesced larger island vibrates, "breezing" more oblate and less in turn. Within the coalesced island the colliding two plasma blobs cause turbulent flows and the originally

directed flow energy quickly dissipates into heat, thereby reducing the amplitude of the temperature oscillations [Fig. 2(a)].

As results of this, the momentum distribution of plasma ions in the poloidal direction shown in Fig. 2(b) exhibit intense bulk heating (including adiabatic heating). The temperature in this direction was increased in our simulation by a factor of 60. The momentum distribution of ions in the toroidal direction [Fig. 2(c)] shows three regimes, the first being the bulk, the second the exponential section $f_2(p_x) = \exp(-p_z/p_0)$, and the third flat distribution up to the relativistic factor $\gamma \sim 2$ in the relativistic region, where $p_0^2/2M \simeq 10 \times$ (bulk temperature). The heating in the poloidal direction is due to the intense process of the adiabatic heating and turbulent dissipation as a result of colliding plasma blobs. The heating in the toroidal direction is due to the heating/acceleration by the inductive toroidal electric field induced by the annihilated poloidal magnetic flux as a result of coalescence.

III. Explanation of Observation

The flare loop slowly expands after it emerges from the photosphere as the toroidal field curvature of the loop makes the centrifugal motion. In time the toroidal current J_t builds up increasing the poloidal magnetic field B_p. As the poloidal field B_p reaches the critical value that is of the order of magnitude B_t, the adjacent flare current loop can now coalesce rapidly facilitated by the fast reconnection process governed by Eq. (1), the faster second phase. Such a fast coalescence of flare current loops proceeds explosively once in its nonlinear regime in a matter of 1-2 Alfven times, releasing more than 1/10 of the poloidal magnetic energy into (ion) kinetic energy. Since the flare loop magnetic field (100G) with current rod size ($a = 10^8$cm), $W_c \sim 0.5 \times 10^{20} \ell n(L/a) \sim 1.5 \times 10^{20}$erg/cm and the energy available in length $d \sim L(\sim 10^9\text{cm})$ is $E = 1.5 \times 10^{29}$erg for $a = 10^8$, $d = L = 10^9$ and $E = 1.5 \times 10^{31}$erg for $a = 10^9$, $d = L = 10^{10}$. Released ion energy, therefore, is $E_{ion} \sim \frac{1}{6} E$ is in between 2×10^{28}erg and 2×10^{30}erg due to the coalescence. This amount of energy is in the neighborhood of the solar flare energy (Sturrock, 1980).

With this magnetic field, the Alfven time is of the order of 1 sec., which is approximately the time scale for explosive coalescence. The time scale of the impulsive phase is observed to be of a second in good agreement with the above theoretical estimate. The sudden nature of the impulsive flare phase (Sturrock, 1980) is thus explained by increasing field aligned current and the faster second phase reconnection in the course of coalescence. The field aligned particle distribution $f(p_z)$ should approximately represent the energy observed in x-rays or γ-rays from flare loop interface with the photosphere

where the energetic particles react with dense photospheric nuclei. Chupp et al.'s observation of these radiation spectra (1974) shows that the soft x-ray energy domain (up to 700keV) and hard x-ray/γ-ray energy domain (up to 7MeV) have different distribution characteristics: in the hard x-ray domain (700 keV-7MeV) the energy spectrum is exponential. This type of characteristics seems to very much match our simulation results, where the particle distribution breaks into the bulk, the e^{-p_z/p_0} domain (energy up to a typical temperature $10 \sim 50$ times of the bulk temperature), and the flat low-population relativistic domain. The amplitude of oscillations in temperature [Fig. 2(a)] along with the periods of the oscillation ($\sim$ 1 Alfven time) and its more minute characteristics astonishingly resemble what is reported of the solar γ-ray amplitude oscillations (Forrest et al., 1981).

Such a sudden heating of ions by the coalescence should increase the plasma pressure in the flare loop, which in turn destabilize the ballooning instability against the flare toroidal fields. This may amount to the plasma mass leakage in the main phase (Kuperus et al., 1967). The coronal x-ray brightening (Svestka et al., 1981) seems to occur due to a similar process. The coalescence of current filaments may also take place in the inside of the flare loop (internal coalescence of magnetic islands). The internal coalescence instability can successively occur, yielding multi-megavolts of ion energy. Such acceleration of ions may happen in the flare main phase, producing solar cosmic ray. The energy range for this (Svestka, 1976) seems plausible by the internal coalescence.

The authors would like to thank Professor E. N. Parker for his helpful discussions. The work was supported by National Science Foundation Grant ATM81-10539 and Department of Energy Grant DE-FG05-80-ET-53088.

REFERENCES

Brunel, F., Leboeuf, J.N., Tajima, T., Dawson, J.M., Makino, M., and Kamimura, T. 1981, J. Comput. Phys. 43, 268.

Brunel, F., Tajima, T., and Dawson, J.M. 1982, Phys. Rev. Lett. submitted for publication.

Chupp, E.L., Forrest, D.J., and Suri, A.N. 1974, in Solar Gamma-, X-, and EUV Radiation (edited by S. Kane) (Reidel, Holland) p. 341.

Forrest, D.J., Chupp, E.L., Ryan, J.M., Reppin, C., Rieger, E., Kanbach, G., Pinkau, K., Share, G., and Kinzer, G. 1981, to be published in the Late Volumes of the 17th International Cosmic Ray Conference; Paris, France.

Furth, H.P., Killeen, J., and Rosenbluth, M.N. 1963, Phys. Fluids. 6, 459.

Howard, R. and Svestka, Z., 1977, Solar Phys. 54, 65.

Kuperus, M. and Tandberg-Hanssen, E. 1967, Solar Phys. 2, 39.

Langdon, A.B. and Lasinski, B.F. 1976, Methods in Computational Physics, Academic, New York, Vol. 16, p. 327.

Leboeuf, J.N., Tajima, T., and Dawson, J.M. 1981, Phys. Fluids, submitted for publication.

Lin, A.T., Dawson, J.M., and Okuda, H. 1974, Phys. Fluids 17, 1995.

Parker, E.N. 1963, Ap. J. Suppl. Ser. 77, 177.

Petschek, H.E. 1964, in Symposium on the Physics of Solar Flares, ed. by W.H. Hess, NASA, Washington, p. 425.

Pritchett, P.L. and Wu, C.C. 1979, Phys. Fluids 22, 440.

Sturrock, P.A. ed. 1980, Solar Flares: Monograph from Skylab Solar Workshop II, Colorado Associated University Press, Boulder.

Svestka, Z. 1976, Solar Flares, Reidel, Holland.

Sweet, P.A. 1958, Nuovo Cimento Suppl. 8 (Ser. 10), 188.

Tajima, T. 1981, Phys. Rev. Lett., submitted for publication.

Wu, C.C., Leboeuf, J.N., Tajima, T., and Dawson, J.M. 1981, Phys. Fluids, submitted for publication.

FIGURE CAPTIONS

Figure 1 - Magnetic field lines showing coalescing two current filaments. (a) taken from a run on MHD particle code (Brunel et al., 1981). System size $L_x \times L_y = 64\Delta \times 64\Delta$ (Δ: grid length), $v_A(y=64\Delta) = 3.6c_s$, (uniform $B_t = 0$), $t = 220\Delta/c_s$. (b)-(d) schematic diagram for fast coalescence based on our simulation. (b) linear stage of coalescence (α: large), (c) nonlinear stage corresponding to (a), (d) late nonlinear stage when faster second phase reconnection sets in (α: larger). c_s is the sound speed.

Figure 2 - Time history of ion temperature during the tearing and coalescence (a) and ion distribution functions after coalescence [(b) and (c)]. Data taken from a run on EM code with system size $L_x \times L_y = 128\Delta \times 32\Delta$ (Δ: grid size), $B_t = 0.2B_p$, $v_A \simeq v_e$(electron thermal velocity), $T_i/T_e = 0.5$(at t=0), mass ratio m/M = 1/10, particle size $a=\Delta$. (a) up to $t = 2\Omega_{ci}^{-1}$ (about $0.5\ t_A$) tearing grows and then saturates. From $t = 22\Omega_{ci}^{-1}$ to $t = 26.5\Omega_{ci}^{-1}$ (in about $2t_A$) the coalescence explosively happens and completes. The period of temperature oscillations is $\sim 2t_A$. (b) ion momentum (p_x) distribution function at $t = 36\Omega_{ci}^{-1}$. (c) toroidal ion momentum (p_z) distribution function at $t = 36\Omega_{ci}^{-1}$. The thermal momenta are indicated by tickmarks near p=0. Momenta are normalized by Mc and $\Omega_{ci} = eB/Mc$.

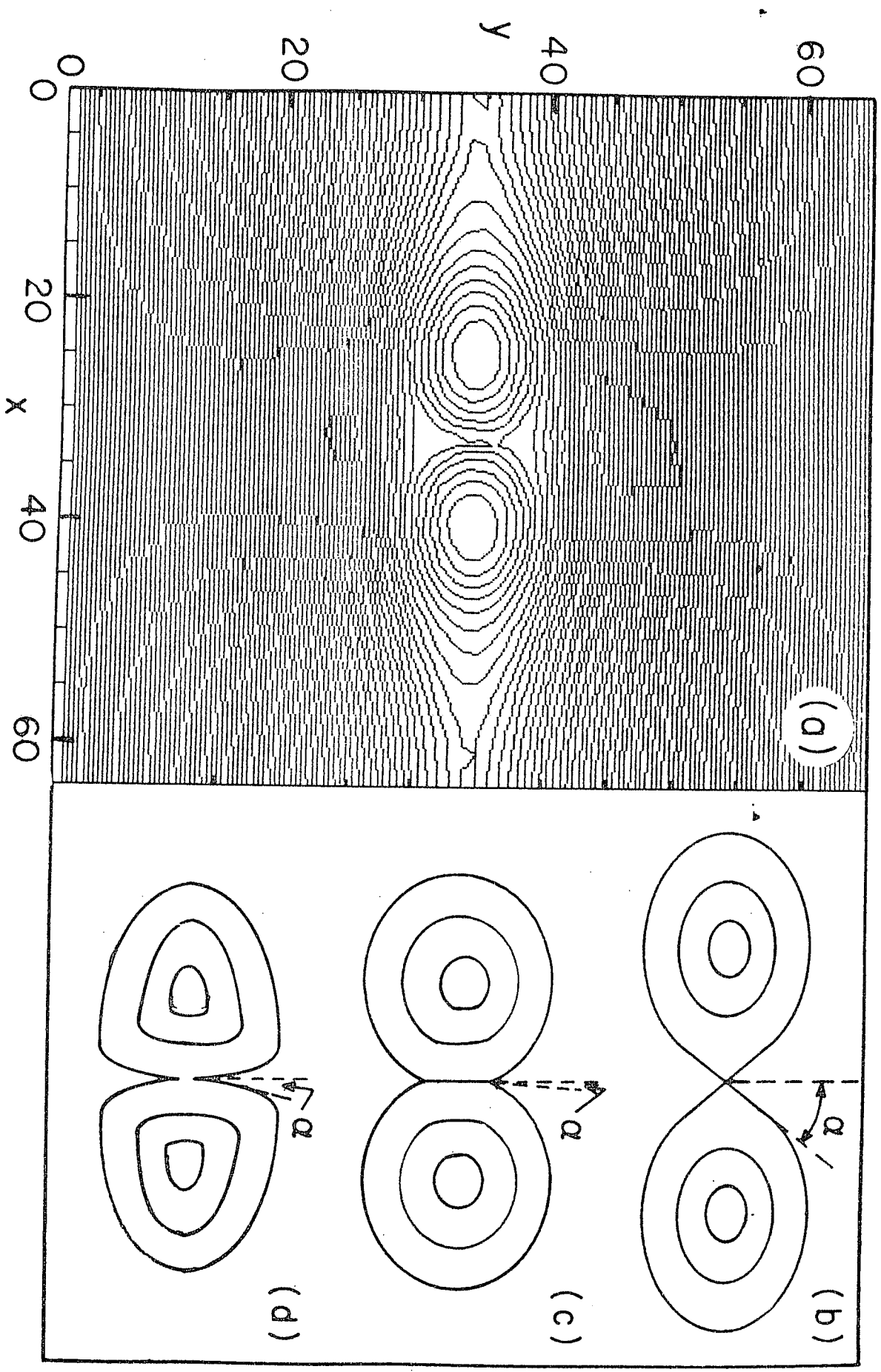

FIG. 1

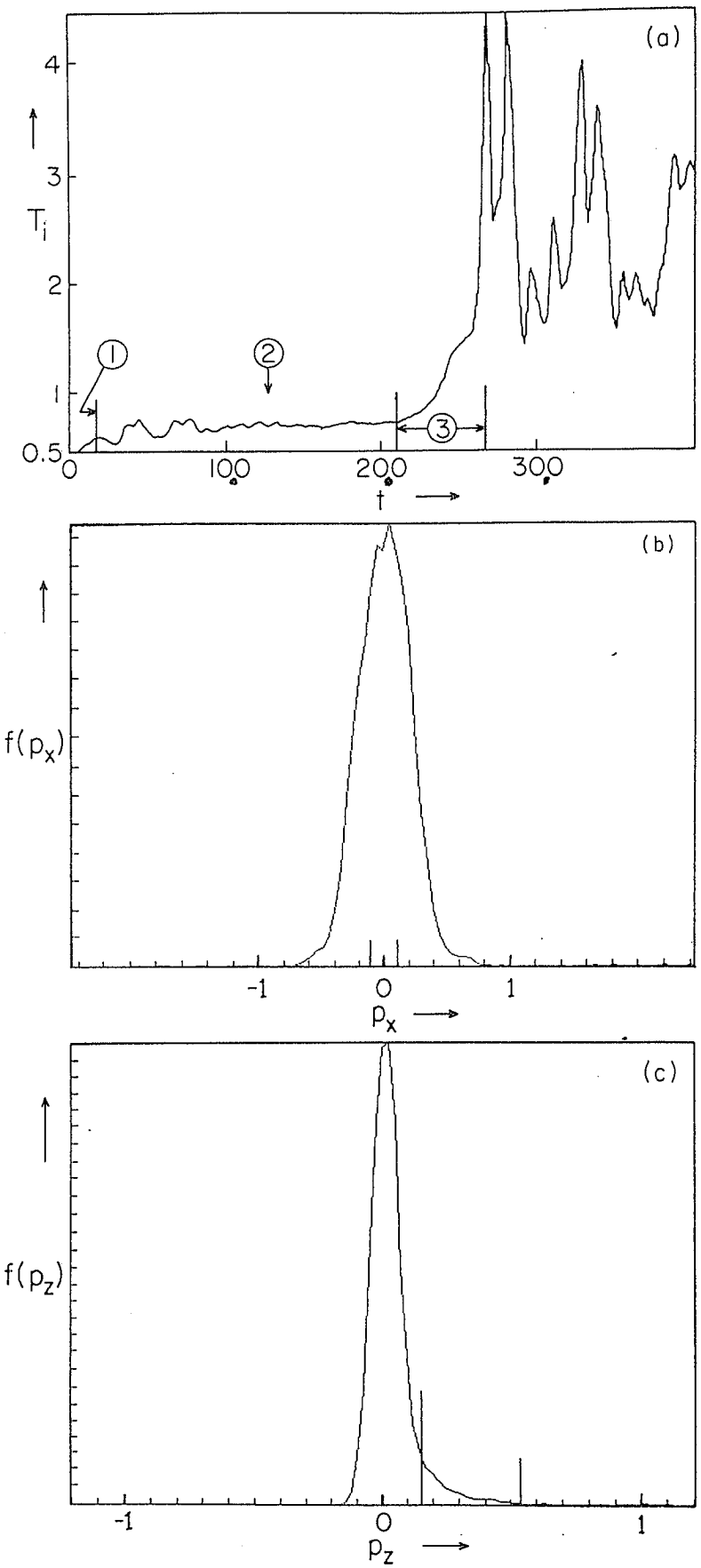

FIG. 2